

## Supporting Information for

### Temporal changes in plasma membrane lipid content induce endocytosis to regulate developmental epithelial-to-mesenchymal transition

Michael L. Piacentino\*, Erica J. Hutchins, Cecelia J. Andrews, and Marianne E. Bronner

\*Corresponding Author: Michael L. Piacentino  
Email: [michaelpiacentino@jhmi.edu](mailto:michaelpiacentino@jhmi.edu)

#### This PDF file includes:

Figures S1 to S5  
Tables S1  
SI References

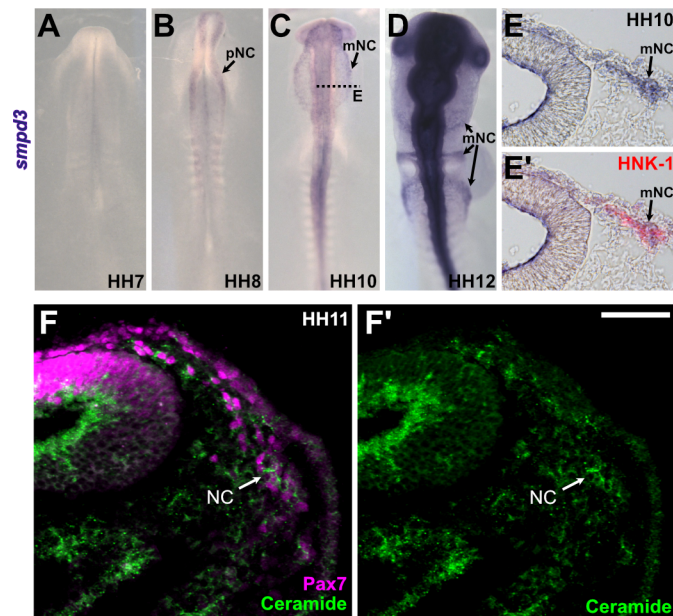


**Fig. S1. *Smpd3* gene expression is detected in premigratory and migratory cranial neural crest cells.** *In situ* hybridization shows that *Smpd3* expression is absent at early stages (A), initiates in specified, premigratory neural crest cells (B), and is maintained during migration (C,D). E, Transverse section of embryos at stage HH10 (C, dashed line) shows *Smpd3* expression in migrating cranial neural crest cells, immunolabeled by the surface antigen HNK-1. HH, Hamburger Hamilton stage; pNC, premigratory neural crest; mNC, migratory neural crest. See also Fig. 1. F, Immunolabeling reveals enrichment of the lipid ceramide in Pax7-labeled migrating neural crest cells at stage HH11, as well as along the apical surface of the neural tube. Scale bar represents 50  $\mu$ m.

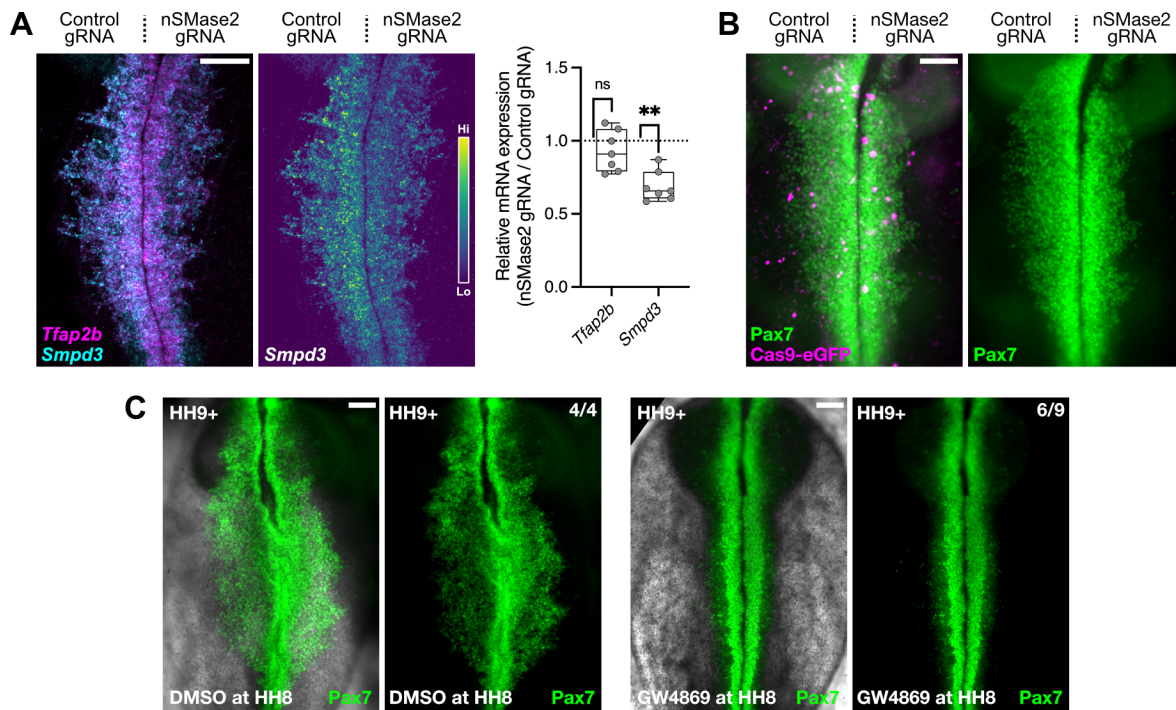


**Fig. S2. CRISPR/Cas9-mediated nSMase2 knockout and neutral sphingomyelinase inhibition phenocopy nSMase2 MO.** **A**, Embryos were electroporated with a Cas9-eGFP-expressing construct, together with U6.3-driven control- or nSMase2-targeting gRNAs. At HH9, embryos were fixed and processed for HCR to detect expression of *Smpd3* transcripts and the neural crest marker *Tfap2b*. Box plot displaying relative fluorescent intensity shows that, compared with control gRNA, nSMase2 gRNA does not affect *Tfap2b* expression but does knock down *Smpd3* transcript levels (n=7 embryos). **B**, Pax7 staining in nSMase2 CRISPR-electroporated embryos reveals a significant reduction in cranial neural crest migration area (See also Fig. 2B for quantitation). **C**, Wild type embryos were treated with DMSO (left) or the neutral sphingomyelinase inhibitor GW4869 (50  $\mu$ m, right) at stage HH8 (prior to neural crest EMT) and incubated until stage HH9+ (migratory stage). Pax7 staining reveals that DMSO treatment did not prevent neural crest EMT (n=4/4), while global GW4869 treatment bilaterally inhibited EMT (n=6/9). Scale bars represent 100  $\mu$ m. ns, non-significant, \*\* $p < 0.01$ ; two-tailed paired *t*-test. See also Fig. 2.

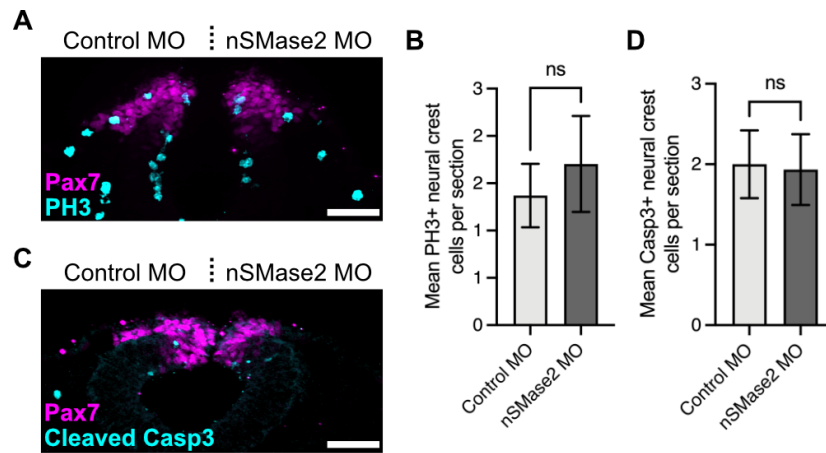


**Fig. S3. nSMase2 knockdown does not affect neural crest proliferation or survival.** Gastrulating chick embryos were electroporated with a non-binding control morpholino (Control MO, left) and nSMase2-targeting morpholino (nSMase2 MO, right), and were subsequently immunostained for the neural crest marker Pax7 and the mitotic marker phospho-histone H3 (PH3, **A**), or for the apoptosis indicator, activated caspase 3 (cleaved Casp3, **C**) in section at the HH9+. Quantitation of PH3+ (n=27 sections from 9 embryos, **B**) and Casp3+ (n=15 sections from 5 embryos, **D**) cells show no significant change between nSMase2 knockdown and the contralateral control. Displayed is the mean with error bars reflecting SEM. Scale bars represent 50  $\mu$ m. ns, non-significant; two-tailed paired *t*-test.

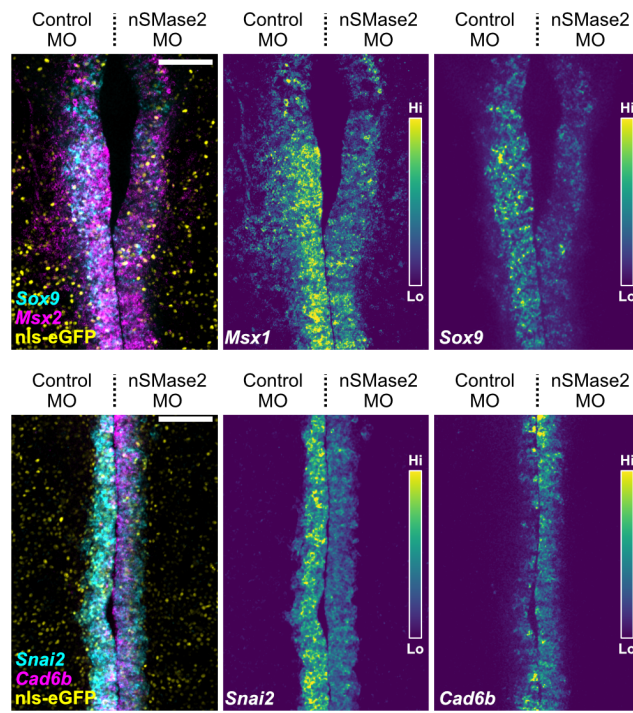


**Fig. S4. nSMase2 knockdown disrupts activation of the EMT transcriptional program.**

Representative images of nSMase2 knockdown embryos co-electroporated with nls-eGFP to label transfected cells, followed by HCR analysis for expression of neural crest markers *Msx1*, *Sox9*, *Snai2*, and *Cad6b* at stage HH9-. Scale bars represent 100  $\mu$ m. See quantitation in Fig. 3A.

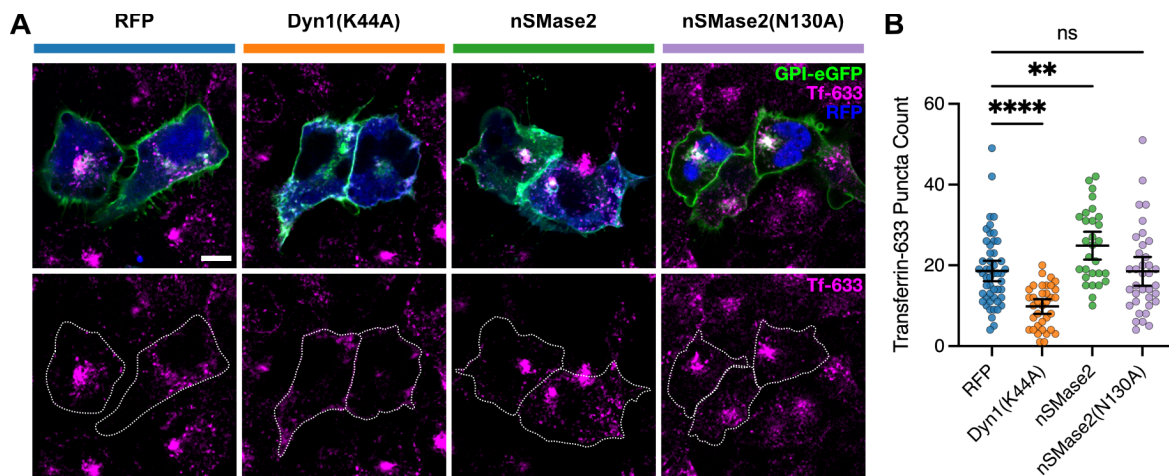


**Fig. S5. nSMase2 catalytic activity is sufficient to induce endocytosis.** **A**, Epithelial cells (U2OS) were transfected with GPI-eGFP to label the plasma membrane and the indicated overexpression constructs. After 24 hours, transfected cells were subjected the Transferrin-633-conjugate endocytosis assays, then fixed and visualized by confocal microscopy. **B**, Dot plot displaying the number of fluorescent Tf-633 puncta within individual transfected cells (n=50 RFP, 35 Dyn1(K44A), 29 nSMase2, and 36 nSMase2(N130A) cells). Overlaid bars display mean and 95% confidence intervals. ns not significant, \*\* $p < 0.01$ , \*\*\*\* $p < 0.0001$ ; one-way ANOVA ( $p < 0.0001$ ) with Dunnett's multiple comparison analysis. White dotted lines indicate cell borders.

**Table S1. Key Resources**

REAGENT or RESOURCE	SOURCE	IDENTIFIER
<b>Antibodies</b>		
Mouse monoclonal IgG1 anti-Pax7	Developmental Studies Hybridoma Bank (DSHB)	Cat# PAX7; RRID:AB_528428
Mouse monoclonal IgM anti-HNK-1	Developmental Studies Hybridoma Bank (DSHB)	Cat# 3H5, RRID:AB_2314644
Mouse monoclonal IgG1 anti-Cad6B	Developmental Studies Hybridoma Bank (DSHB)	Cat# CCD6B-1, RRID:AB_531766
Rabbit monoclonal anti-Laminin (LAMA1)	Sigma-Aldrich	Cat# L9393, RRID:AB_477163
Rabbit polyclonal anti-Sox9	Millipore	Cat# AB5535, RRID:AB_2239761
Mouse monoclonal IgG1 anti-FLAG (Clone M2)	Sigma-Aldrich	Cat# F1804, RRID: AB_262044
Mouse monoclonal IgM anti-Ceramide (Clone MID 15B4)	Sigma-Aldrich	Cat# C8104, RRID:AB_259087
Rabbit polyclonal anti-phospho-Histone H3 (Ser10)	Millipore	Cat# 06-570, RRID:AB_310177
Rabbit polyclonal anti-Caspase-3, activated form	R & D Systems	Cat# AF835, RRID:AB_2243952
Rabbit monoclonal anti-Slug (Snai2, Clone C19G7)	Cell Signaling Technologies	Cat# 9585, RRID:AB_2239535
Goat polyclonal anti-GFP	Rockland	Cat# 600-101-215M, RRID:AB_2612804
Rabbit polyclonal anti-RFP/DsRed	MBL International	Cat# PM005, RRID:AB_591279
<b>Chemicals, Peptides, and Recombinant Proteins</b>		
Chemical: GW4869	Sigma-Aldrich	Cat# D1692
Peptide: Transferrin from Human Serum, Alexa Fluor 633 Conjugate	ThermoFisher Scientific	Cat# T23362
Dextran, Alexa Fluor 488; 3,000 MW, Anionic	ThermoFisher Scientific	Cat# D34682
C12 Ceramide (d18:1/12:0)	Avanti Polar Lipids	Cat# 860512
<b>Deposited Data</b>		
Bulk RNA-Seq: FACS-isolated chicken cells (neural crest at 5-6 somite stage, 8-10 somite stage, non-neural crest)	(1)	BioProject: PRJNA497574
Bulk RNA-Seq: Dissected chicken somites (epithelial somite stage, maturing somite stage)	(2)	BioProject: PRJNA602335
<b>Experimental Models: Cell Lines</b>		
Human: U2OS Cell Line	ATCC	Cat# HTB-96, RRID:CVCL_0042
<b>Experimental Models: Organisms/Strains</b>		
Fertilized chicken eggs	Sunstate Ranch, Sylmar, CA	

Fertilized chicken eggs	AA Laboratory Eggs, Westminster, CA	
<b>Oligonucleotides</b>		
Morpholino: Control MO CCTCTTACCTCAGTTACAATTTATA	Gene Tools	N/A
Morpholino: nSMase2 MO GGTGCACTGTGTCAAGCATCCATA	Gene Tools	N/A
CRISPR/Cas9 gRNA Target: Control GCACTGCTACGATCTACACC	(3)	N/A
CRISPR/Cas9 gRNA Target: <i>SMPD3</i> GCAATCTGCGCAGCCCGAGA	This paper	N/A
Primer: nSMase2 FWD -76: CCTCAGTGTGCTATGGATGC	This paper	N/A
Primer: nSMase2 REV 894 T7: TAATACGACTCACTATAGGGAAGTCCAGAAATCTCC ATCC	This paper	N/A
Primer: nSMase2 ATG XhoI: ATATCTCGAGGCCACCATGGTTTTATATACTTCCCC AT	This paper	N/A
Primer: nSMase2 stop ClaI: ATATATCGATTAAAGGATCATCTTCTCCTGTAG	This paper	N/A
Primer: nSMase2 N130A REV: GCAGCAGGCAAACGGCGCACTGCCAAAGC	This paper	N/A
Primer: nSMase2 N130A FWD: GCTTTGGCAGTGCCGCCGTTTGCCTGCTGC	This paper	N/A
Primer: nSMase2 2462 REV: CATGCTACTGATGCAAGCACG	This paper	N/A
Primer: nSMase2 ATG SphI: TAGAGCATGCTATTATGCCACCATGGTTTTATATAC	This paper	N/A
Primer: nSMase2 nostop ClaI: CTCCATCGATTCTCTCCAGGATCATCTTCTCCTG TAGAC	This paper	N/A
Primer: nSMase2 FLAG ClaI: GCTTATCGATTCACTTGTGTCATCGTCTTTGTAGTC GCCGGAGCCAGGATCATCTTCTCCTGTAG	This paper	N/A
Primer: LRP6 Signal Peptide FWD: TTTGGCAAAGAATTGCTCGAGCCACCATGGGGGCC GTCCTGAGGAG	This paper	N/A
Primer: LRP6 Signal Peptide FLAG REV: GCAACAAAGGCTTGTGTCATCGTCTTTGTAGTCCA ACAAAGGGGCCGCTCTCA	This paper	N/A
Primer: LRP6 FLAG FWD: GCAACAAAGGCTTGTGTCATCGTCTTTGTAGTCCA ACAAAGGGGCCGCTCTCA	This paper	N/A
Primer: LRP6 REV: ATTGATATCAAGCTTATCGTCAGGAGGAGTCTGTA CAGG	This paper	N/A
<b>Recombinant DNA</b>		
Plasmid: pCl::nSMase2	This paper	N/A
Plasmid: pCl::nSMase2-FLAG	This paper	N/A
Plasmid: pCl::nSMase2(N130A)	This paper	N/A
Plasmid: pCAG::nSMase2-RFP	This paper	N/A
Plasmid: pCAG::2a-RFP	(4)	N/A
Plasmid: pCl::H2B-RFP	(5)	N/A



Plasmid: pCl::nls-GFP	(6)	N/A
Plasmid: CMV::Dyn1(K44A)-mRFP	(7)	Addgene plasmid #55795
Plasmid: pTK- <i>FoxD3</i> -NC1.1m3::GFP	(8)	N/A
Plasmid: pTK- <i>FoxD3</i> -NC1.1m3::Dyn1(K44A)-mRFP	This paper	N/A
Plasmid: pCAG::GPI-eGFP	(9)	Addgene plasmid #32601
Plasmid: PM-eGFP	(10)	Addgene plasmid #21213
Plasmid: pCAG::PM-eGFP	This paper	N/A
Plasmid: TCF/Lef::GFP	(11)	Addgene plasmid #32610
Plasmid: M38-TOP::d2EGFP	Laboratory of Randall Moon	Addgene plasmid #17114
Plasmid: TCF/Lef::H2B-d2EGFP	This paper	N/A
Plasmid: BRE::GFP	(12)	N/A
Plasmid: BRE::H2B-d2EGFP	(4)	N/A
Plasmid: CMV::VSVG-LRP6	(13)	N/A
Plasmid: pCl::FLAG-LRP6	This paper	N/A
Plasmid: pCAG::Cas9	(3)	Addgene plasmid #99138
Plasmid: U6.3::empty	(3)	Addgene plasmid #99139
Plasmid: U6.3::Control gRNA	(3)	Addgene plasmid #99140
Plasmid: U6.3::SMPD3 gRNA	This paper	N/A

### Software and Algorithms

Fiji v1.53c	(14)	<a href="https://imagej.net/Fiji">https://imagej.net/Fiji</a>
Bowtie2 v2.3.5.1	(15)	<a href="http://bowtie-bio.sourceforge.net/bowtie2/index.shtml">http://bowtie-bio.sourceforge.net/bowtie2/index.shtml</a>
Cutadapt v2.10	(16)	<a href="https://cutadapt.readthedocs.io/en/stable/">https://cutadapt.readthedocs.io/en/stable/</a>
FeatureCounts v2.0.1	(17)	<a href="http://subread.sourceforge.net/">http://subread.sourceforge.net/</a>
R v3.6.1	(18)	<a href="https://www.r-project.org/">https://www.r-project.org/</a>
RStudio v1.2.1335	(19)	<a href="https://www.rstudio.com/">https://www.rstudio.com/</a>
DESeq2	(20)	<a href="https://bioconductor.org/packages/release/bioc/html/DESeq2.html">https://bioconductor.org/packages/release/bioc/html/DESeq2.html</a>
Python v3.7.6	(21)	<a href="https://www.python.org/downloads/release/python-376/">https://www.python.org/downloads/release/python-376/</a>
Pandas v0.24.2	(22)	<a href="https://pandas.pydata.org/">https://pandas.pydata.org/</a>
Bokeh v1.4.0	(23)	<a href="https://docs.bokeh.org/en/latest/index.html">https://docs.bokeh.org/en/latest/index.html</a>
iqplot v0.1.6	(24)	<a href="https://iqplot.github.io/index.html">https://iqplot.github.io/index.html</a>
Scipy v1.5.2	(25)	<a href="https://scipy.org/">https://scipy.org/</a>

Scikit_posthoc v0.6.5	(26)	<a href="https://scikit-posthocs.readthedocs.io/en/latest/">https://scikit-posthocs.readthedocs.io/en/latest/</a>
Numpy v1.19.2	(27)	<a href="https://numpy.org/devdocs/index.html">https://numpy.org/devdocs/index.html</a>
Seaborn v0.11.0	(28)	<a href="https://seaborn.pydata.org/">https://seaborn.pydata.org/</a>
Holoviews v1.13.3	(29)	<a href="https://holoviews.org/">https://holoviews.org/</a>
GraphPad Prism 9 v9.2.0(283)		<a href="https://www.graphpad.com/">https://www.graphpad.com/</a>

## SI References

1. R. M. Williams, *et al.*, Reconstruction of the Global Neural Crest Gene Regulatory Network In Vivo. *Dev. Cell* **51**, 255-276.e7 (2019).
2. G. F. Mok, *et al.*, Characterising open chromatin in chick embryos identifies cis-regulatory elements important for paraxial mesoderm formation and axis extension. *Nat. Commun.* **12**, 1157 (2021).
3. S. Gandhi, M. L. Piacentino, F. M. Vieceli, M. E. Bronner, Optimization of CRISPR/Cas9 genome editing for loss-of-function in the early chick embryo. *Dev. Biol.* **432**, 86–97 (2017).
4. M. L. Piacentino, E. J. Hutchins, M. E. Bronner, Essential function and targets of BMP signaling during midbrain neural crest delamination. *Dev. Biol.* **477**, 251–261 (2021).
5. P. Betancur, M. Bronner-Fraser, T. Sauka-Spengler, Genomic code for Sox10 activation reveals a key regulatory enhancer for cranial neural crest. *Proc. Natl. Acad. Sci. U. S. A.* **107**, 3570–3575 (2010).
6. S. G. Megason, A. P. McMahon, A mitogen gradient of dorsal midline Wnts organizes growth in the CNS. *Development* (2002).
7. T. R. Hynes, S. M. Mervine, E. A. Yost, J. L. Sabo, C. H. Berlot, Live cell imaging of Gs and the beta2-adrenergic receptor demonstrates that both alphas and beta1gamma7 internalize upon stimulation and exhibit similar trafficking patterns that differ from that of the beta2-adrenergic receptor. *J. Biol. Chem.* **279**, 44101–44112 (2004).
8. M. S. Simões-Costa, S. J. McKeown, J. Tan-Cabugao, T. Sauka-Spengler, M. E. Bronner, Dynamic and differential regulation of stem cell factor FoxD3 in the neural crest is Encrypted in the genome. *PLoS Genet.* **8**, e1003142 (2012).
9. J. M. Rhee, *et al.*, In vivo imaging and differential localization of lipid-modified GFP-variant fusions in embryonic stem cells and mice. *Genesis* **44**, 202–218 (2006).
10. M. N. Teruel, T. A. Blanpied, K. Shen, G. J. Augustine, T. Meyer, A versatile microporation technique for the transfection of cultured CNS neurons. *J. Neurosci. Methods* **93**, 37–48 (1999).
11. A. Ferrer-Vaquer, *et al.*, A sensitive and bright single-cell resolution live imaging reporter of Wnt/ $\beta$ -catenin signaling in the mouse. *BMC Dev. Biol.* **10**, 121 (2010).
12. G. Le Dréau, *et al.*, Canonical BMP7 activity is required for the generation of discrete neuronal populations in the dorsal spinal cord. *Development* **139**, 259–268 (2012).
13. B. T. MacDonald, M. V. Semenov, H. Huang, X. He, Dissecting molecular differences between Wnt coreceptors LRP5 and LRP6. *PLoS One* **6**, e23537 (2011).
14. J. Schindelin, *et al.*, Fiji: an open-source platform for biological-image analysis. *Nat. Methods* **9**, 676–682 (2012).
15. B. Langmead, S. L. Salzberg, Fast gapped-read alignment with Bowtie 2. *Nat. Methods* **9**, 357–359 (2012).

16. M. Martin, Cutadapt removes adapter sequences from high-throughput sequencing reads. *EMBnet.journal* **17**, 10–12 (2011).
17. Y. Liao, G. K. Smyth, W. Shi, featureCounts: an efficient general purpose program for assigning sequence reads to genomic features. *Bioinformatics* **30**, 923–930 (2014).
18. R. Ihaka, R. Gentleman, R: A Language for Data Analysis and Graphics. *J. Comput. Graph. Stat.* **5**, 299–314 (1996).
19. J. S. Racine, RSTUDIO: A platform-independent IDE for R and sweave. *Journal of Applied Econometrics* **27** (2012).
20. M. I. Love, W. Huber, S. Anders, Moderated estimation of fold change and dispersion for RNA-seq data with DESeq2. *Genome Biol.* **15**, 550 (2014).
21. G. van Rossum, F. L. Drake, *Python 3 Reference Manual* (2009).
22. W. McKinney, P. D. Team, Pandas-Powerful python data analysis toolkit. *Pandas—Powerful Python Data Analysis Toolkit* **1625** (2015).
23. Bokeh Development Team, *Bokeh: Python library for interactive visualization* (2018).
24. J. S. Bois, justinbois/iqplot: 0.1.6 (2020) <https://doi.org/10.22002/D1.1614>.
25. P. Virtanen, *et al.*, SciPy 1.0: fundamental algorithms for scientific computing in Python. *Nat. Methods* **17**, 261–272 (2020).
26. M. Terpilowski, scikit-posthocs: Pairwise multiple comparison tests in Python. *J. Open Source Softw.* **4**, 1169 (2019).
27. S. van der Walt, S. C. Colbert, G. Varoquaux, The NumPy Array: A Structure for Efficient Numerical Computation. *Computing in Science Engineering* **13**, 22–30 (2011).
28. M. Waskom, seaborn: statistical data visualization. *J. Open Source Softw.* **6**, 3021 (2021).
29. J.-L. Stevens, P. Rudiger, J. Bednar, HoloViews: Building complex visualizations easily for reproducible science in *Proceedings of the 14th Python in Science Conference*, (SciPy, 2015) <https://doi.org/10.25080/majora-7b98e3ed-00a>.